# Landscape Characterization using Geomorphometric Parameters for a Small Sub-Humid River Basin of the Chota Nagpur Plateau, Eastern India

**6**

Jayesh Mukherjee and Priyank Pravin Patel

## Abstract

River responses to endogenic perturbations and climatic attributes lead to the morphological development of basins, the quantification of whose terrain facets to decipher the ambient process-response mechanisms has long been an important aspect of geomorphological studies. The availability of newer, higher resolution datasets, however, entail that past exercises in this domain be looked at anew, in terms of the greater sensitivity and diversity of information that can now be extracted/collated. Here, we combine classical and modern morphometric methods to examine the terrain characteristics of the Kharkai River Basin in eastern India, with this basin chosen for its diversity of landforms and human activities. While traditional methods have been based on eliciting terrain information from topographical maps, we use a higher resolution Digital Elevation Model (DEM) to extract such attributes. The stream network was derived using flow-routing and flow accumulation algorithms and a net of 1 km × 1 km grids was overlain on the DEM to compute various morphometric parameters. These were combined using Principal Component Analysis to demarcate distinct physiographic/landscape entities, in conjunction with the corresponding lithological and soil attributes of the area. Multi-temporal land cover and land use layers extracted from Landsat datasets were overlain on the extracted terrain units to estimate changes in the same across different landscape types. The demarcated terrain units strongly correlated with the lithology, as expected, and this also controlled local slope and drainage development. More rugged locales had greater vegetation cover but were also threatened by deforestation due to agricultural expansion and mining.

## 6.1 Introduction

The term 'Morphometry' was initially adopted by De Martonne (1934), and 'morphometric methods' encapsulate the numerical characterization of different landform/landscape attributes/elements as enumerated from digital elevation datasets or

J. Mukherjee · P. P. Patel (✉)
Department of Geography, Presidency University, 86/1, College Street, Kolkata, West Bengal 700073, India
e-mail: priyank.geog@presiuniv.ac.in

J. Mukherjee
Centre for the Study of Regional Development, School of Social Sciences, Jawaharlal Nehru University, New Delhi 110067, India

from topographical maps. Morphometry, then is widely considered as the mathematical measurement of the Earth's surface together with the shape, dimension and distribution of its constituent landforms (Clarke 1996; Agarwal 1998; Obi Reddy et al. 2002; Vaidya et al. 2013; Singh et al. 2014; Asfaw et al. 2019). This provides the basis for 'quantitative geomorphology' and as such can be viewed as the means of creating a 'census handbook of the landform' with a purpose to provide an empirical description of its inherent characteristics without delving into or trying to formulate a hypothesis of its origin. The main aspects of the landform features which provide the differentiating characteristics and which can be studied from a topographical map are (Hammond 1954)—the area (surface arrangement), altitude, relief and volume (horizontal dimension) and the slope (deviation of the surface from the horizontal). All these individual elements, along with the overall different aspects of the drainage basin within which they are situated, are investigated in morphometric examinations and terrain analysis.

The eventual aim of these analyses is *terrain characterization leading to terrain modelling* (Patel and Sarkar 2010), not only to decipher just the general surface attributes but also garnered towards any type of geo-applications. Investigating such indicators helps reveal the geo-hydro morphological functioning of drainage basins (Horton 1945; Evans 1972, 1984), which encapsulates ambient factors like climate, topography (Strahler 1952, 1964; Chorley et al. 1984), structure (Shreve 1969; Merritts and Vincent 1989; Oguchi 1997), tectonics and its geomorphology (Mueller 1968; Ohmori 1993; Cox 1994; Burrough and McDonnell 1998; Hurtrez et al. 1999). Hence, such attributes are crucial factors in gauging landscape evolution (Goodbred 2003; Das et al. 2018a) and profoundly impact the basin network (Zhang 2005; Das et al. 2018b) developed within a watershed. The combined assessment of these characteristics successfully mirror the overall denudational evolution of a locale (Patel et al. 2021). Thus, any landscape is readily explainable with the help of morphometry, in terms of architectural unevenness and watershed characteristics, that together with the underlying hydro-geological processes have been operative in creating the present landforms (Horton 1932; Smith 1958; Miller 1953; Soni 2017; Gizachew and Berhan 2018; Asfaw et al. 2019), and in enabling soil erosion and other surficial processes (Khare et al. 2014; Asfaw et al. 2019).

Thus *geomorphometry* intertwines principles from mathematics, computer science and earth system analysis (or simple morphometry). This field has been revolutionized by geocomputational advances over the last three decades and the greater development and availability of coarser and higher resolution digital elevation models (DEMs) (Maune 2001). Morphometric exercises are now largely undertaken through various geographic information systems (GIS) or dedicated software suites. Newer remotely sensed datasets and relevant methods have simplified terrain and hydro-morphometric analyses of drainage basins from DEMs (Jensen 1991; Wise 2000; Aparna et al. 2015; Patel 2013; Patel et al. 2016; Gutema et al. 2017; Gizachew and Berhan 2018; Kabite and Gessesse 2018; Afsaw et al. 2019). Harinath and Raghu (2013) have further explained how in situ methods of landscape and terrain evaluation are laborious, time consuming and capital intensive, while geomorphometric analysis provides far easier evaluative measures of drainage basins.

However, continuously representative surfaces are hard to characterize using traditional measures and newer various parameters have been framed to enumerate terrain facets that older measures may fail to describe. Two such methods are the 'terrain fabric' (Guth 2001) and the surface 'openness' (Yokoyama 2002) parameters. Terrain fabric characterization is the probability that a surface is organized as linear ridges rather than as isotropic topography, while openness reveals the dominance of exposure over enclosure of a site. Yet many computed variables are similar in nature, e.g. the hypsometric integral and elevation skewness parameters are quite similar (Pike 2001). Currently, DEM analysis could be best termed as 'a modern, analytical, cartographic approach to represent the bare-earth topography by the computer manipulation of terrain heights' (Tobler 2000).

Landscape interlinkages form the basic foundation of the economy in most developing countries, encapsulated by its water and land attributes (Chattopadhyay and Carpenter 1990). Surface drainage characteristics have been quantified and mapped worldwide, mostly employing traditional methods (e.g. Horton 1945; Morrisawa 1959; Langbein and Leopold 1964; Strahler 1954, 1957, 1964). Such analyses have aimed to assess drainage properties by measuring various channel network aspects, e.g. stream ordering, watershed area and perimeter extents, drainage length, density and frequency, bifurcation and texture ratios (Kumar et al. 2000), to mention but a few. For such quantitative characterization of a watershed, measurements of linear/areal aspects, stream gradients and valley slopes are required (Kumar et al. 2000; Nag and Chakraborty 2003; Krishnamurthy 1996; Vijith and Satheesh 2006). These analyses help reveal the ambient drainage character and its interactions with the local topography (Obi Reddy et al. 2002, 2004; Sutradhar 2020).

The underlying geology, exogenic and endogenic processes and major climatic alterations profoundly influence drainage network development (Ghosh 2016), the genesis and morphology of landforms, soil properties and the alterations in present-day land use and land cover due to both natural and anthropogenic stimuli, causing degradation (Subhramanyan 1981; Javed et al. 2009, 2011; Altaf et al. 2014; Islam and Barman 2020). Morphometric aspects are thus used in various catchment-based assessments like terrain analysis (Patel and Sarkar 2010), delineation of geomorphological features, quantitative geomorphology and watershed prioritization (Sarkar and Patel 2011, 2012).

The novelty of this research is its combining of traditional and the modern morphometric techniques to bridge the remaining gaps found across the literatures that either use the newer or the more conventional morphometric techniques to explain river basin landscapes. This work underlines the multi-temporal alterations observed along different topographic classes occurring over various morphogenetic regions using statistical measure like factor score, which helps to decipher a new comparative way of investigating and comprehending the river basin landscape. This in turn will also help to identify those areas in urgent need of attention in terms of effectuating proper land and water preservation exercises.

The major objectives of the present research thus include extraction and exploration of the structural properties of the Kharkai River basin, underlining its terrain aspects using conventional grid-based morphometry and more recent GIS-based automated algorithms. The second objective is to understand the relation between the geomorphometric parameters using statistical measures like Principal Component Analysis (PCA) to delineate distinct terrain units present within the basin, highlighting their erodibility and validating the results obtained from geomorphometric evaluation. The final objective is to bring out the multi-temporal changes occurring within the river basin by detecting the land use and land cover (LULC) alterations across the past thirty years, which would help pinpoint areas that need attention for implementing land and water conservation practices.

## 6.2  Materials and Methods

### 6.2.1  Database

The methodology followed in this study requires diverse datasets from four main sources—the remotely sensed SRTM DEM (Shuttle Radar Topographic Mission Digital Elevation Model) tiles and the LANDSAT imageries of the study area from the Earth Explorer repository of the USGS (United States Geological Survey) (https://earthexplorer.usgs.gov/); Survey of India topographical maps for corroboration of river basin outline and DEM-extracted stream network; and finally geology, lithology and geomorphology maps from the Geological Survey of India quadrangles. Table 6.1 lists the data types and their respective sources in detail.

**Table 6.1** Enumerated list of parameters in the present study

| Sl. No | Parameters | Data type | Data source | Scale/resolution | Time period |
|---|---|---|---|---|---|
| 1. | Elevation, Terrain & Drainage | Raster | SRTM DEM (USGS), version 3.0 | 30 m | September, 2014 |
| 2. | Topography & Kharkai River Channel | Line and polygon coverage | Survey of India Topographical Maps, Sheet Numbers—73F/5, F/6, F/7, F/9, F/10, F/11, F/12, F/13, F/14, F/15, F/16; 73 J/2, J/3, J/4, J/7, J/8; 73 K/1 and K/5 | 1:50,000 | 2006 |
| 3. | Geology & Lithology | Polygon coverage | Geological Survey of India Quadrangles | 1:250,000 | 2006 |
| 4. | Geomorphology | Polygon coverage | Geological Survey of India Quadrangles | 1:250,000 | 2006 |
| 5. | Land use & Land cover | Raster | Landsat TM 4–5 C-1 Level-1 and Landsat 8 OLI/TIRS C1 Level 1; Paths/Rows: 140−44 & 140−45 | 30 m | December, 1990 & April, 2020 |

## 6.2.2 Data Analysis

The analysis undertaken was to primarily extract the terrain information on various GIS platforms like MapInfo Professional GIS and ArcMap 10.3, while other allied mapping and statistical software like Whitebox GAT-3.4, SAGA GIS 7.5 and IBM SPSS-23 were used for creating the geo-database. Terrain aspects and drainage networks were demarcated and extracted and then the attribute data pertaining to the stream and basin parameters were attached accordingly to generate the required database for producing the maps. Three-dimensional (3-D) surfaces of relevant geomorphic parameters of the basin were subsequently generated and the respective isopleth maps prepared. Map overlays were done to show spatial relations between different attributes. The empirical relationships derived between the various morphometric variables—liner, areal, relief attributes enabled terrain classification for demarcating distinct physiographic units within the basin using PCA-based factor analysis and hierarchical clustering. These were validated and correlated with the existent LULC types and patterns.

## 6.2.3 Extraction of Morphometric Parameters

Following conventional practice, the entire river basin was covered by grids of 1 km × 1 km dimension for extraction of the morphometric attributes for each grid and this starts with the visual analysis of the DEM surface to distinguish various relief features (Patel 2012). This was followed by the correlation of the ascertained relief features with the basin geology by draping the litho-cover map over the DEM surface and the generation of contours at 10 m interval. The extraction of stream networks using the D8 method of flow routing and flow accumulation methods then followed, with this eliciting a more denser river network than is usually obtainable from topographical maps (Patel and Sarkar 2009; Das et al. 2016). The grid-wise extraction of various morphometric parameters like *maximum grid elevation, mean grid elevation, relative relief, average slope, dissection index, stream frequency, hypsometric integral surrogate, drainage density and texture and ruggedness index* was done subsequently. Through interpolation of the extracted parameter values from the centroid

of each morphometric grid using triangulation technique- inverse distance weighted (IDW), the respective isoline maps were generated. Computation of numbers of grids and amount of basin area falling under the respective iso-zones in each isoline map generated above led to the preparation of frequency or percentage area histograms on this basis. The other terrain morphometric parameters such as *terrain surface texture, terrain surface convexity, topographical wetness index and topographical position index* were calculated based on automated algorithms which are already coded in a GIS environment and can thus be extracted directly from the input DEM tiles. Brief explanations of the enumerated parameters are as follows:

- **Mean elevation**: The average altitude within each grid is recorded on the basis of enumeration of all the DEM pixels falling within it.
- **Relative relief**: Considered as the 'amplitude of available relief' or 'local relief', it is the elevation difference between the lowest and highest points in an areal unit (Smith 1935).
- **Average slope**: Slopes (the angular terrain inclinations between the ridge crest and valley bottom) result from the combination of the local geological structure, absolute/relative relief, vegetation cover, climate, drainage and degree of dissection. It is a vector quantity and Wentworth (1930) put forward a method for the calculation of the average slope of an area (in degrees). In this method, however, the counting of contour crossings does not strictly take into account the nature of the gradient since the same contour may cut a grid on numerous occasions and thus a higher slope value will be obtained which is not actually the case. Furthermore, the sensitivity of the derived slope value is dependent on the contour interval and the smaller the contour interval, the better minor gradient changes can be enumerated.
- **Dissection index**: It is the ratio of the relative relief and the highest elevation in a grid, and indicates the dissection/magnitude of a terrain. 'It takes into account the dynamic potential state of the area as well, i.e., the ratio between relative relief (relief energy) and the perpendicular distance from the erosion base' (Miller 1953; Nir 1957). The classification of the dissection index values is as follows (modified from Kumar and Pandey 1982): less dissected (below 0.1), medium dissected (0.1–0.3), much dissected (0.3–0.6), highly dissected (above 0.6). The values for the dissection index so derived vary between 0 (when the entire depth of altitude is dissected) and 1 (where minimum altitude is equal to the maximum altitude—no dissection has taken place). It reveals gently rolling uplands and dissections in mountainous areas particularly (Pal 1972). This index can be indicative of the erosional cycle stage, with old, mature and young stages related to dissection values.
- **Hypsometry surrogate**: The grid-wise Hypsometric Integral (HI) was computed across the basin surface as proposed by Pike and Wilson (1971).
- **Terrain Surface Texture**: Terrain textures consider relief (Z factor) and spacing (X, Y factors), which represent measures of spatial intricacy per unit area, incorporating the drainage density and slope curvature. This measure highlights the 'fine-versus coarse expression of topographic spacing', i.e. the 'grain' (Ayalew and Yamagishi 2004; Iwahashi and Pike 2007), and was earlier referred to as 'frequency of valleys and ridges' or 'roughness' (Iwahashi 1994; Iwahashi and Kamiya 1995; Iwahashi et al. 2001).
- **Terrain Surface Convexity**: For automatic classification of a high gradient topography, slope gradient and surface texture of the topography play a combinational and fundamental role, but are inadequate to classify low relief features, for instance, segregating older river terraces from the younger ones. So in order to better demarcate these, the local convexity or positive surface curvature was utilized by Iwahashi and Pike (2007). It is commonly seen that low surface convexity conforms to broad valleys and mountain foot slopes, while higher values are typically associated features like alluvial fans or terraces.

- **Topographical Wetness Index**: The TWI parameter measures the relief effect on the generation of runoff (O'Loughlin 1986) and thereby approximates surface saturation zones (Beven and Kirkby 1979; Barling et al. 1994). Similar TWI value zones are likely to behave in a similar hydrological manner when precipitation occurs, if the other ambient conditions match (Qin et al. 2011). The TWI depends on the algorithms used to compute the upslope contributing area and the slope gradient (Qin et al. 2009).

- **Topographical Position Index**: The TPI parameter (Guisan et al. 1999) is an automated algorithm meant for measuring topographic slope positions and enable landform classification. It has been used in geology (Mora-Vallejo et al. 2008; Deumlich et al. 2010; Illés et al. 2011), geomorphology (Tagil and Jenness 2008; Liu et al. 2009; McGarigal et al. 2009; De Reu et al. 2013), hydrology (Lesschen et al. 2007; Francés and Lubczynski 2011; Liu et al. 2011) and many more to such allied branches and quantifies the elevation difference of a central point and the mean elevation within a predetermined radius from it (Gallant and Wilson 2000; Weiss 2000, 2001). Positive TPI values are discerned for central point that are located above their surroundings, and negative values indicate lower topographic positions. The TPI range thus depends on the predetermined radius and elevation difference (e.g. Grohmann and Riccomini 2009). Higher predetermined radius values usually denote major landforms while lower values correspond to minor valleys and ridges (De Reu et al. 2013).

- **Stream frequency**: It denotes the total number of streams flowing per unit area (Horton 1945) and is closely related with the drainage density, and the various parameters that influence drainage density. It is indicative of the nature of runoff in an area, giving insights into the overland flow length and channel spacing. To compute it, all drainage lines were clipped using each morphometric grid and the number of channel segments lying within each grid were counted. The sum of the length of each

of these drainage lines is later used while computing the grid-wise drainage density.

- **Drainage density**: Horton (1945) enumerated this as the ratio of the sum of all stream lengths within the basin to its total area. As a principal component of the landscape that could be investigated using maps and aerial photographs, drainage density has been the subject of numerous studies with the underlying belief being that if the numerous independent variables that control drainage density could be quantitatively related to it, the results would be of great academic interest and practical value (Schumm 1956; Lin and Oguchi 2004). Thus, it is an important variable that has been related to climate change (Rodriguez-Iturbe and Escobar 1982; Moglen et al. 1998), slope failure (Oguchi 1997), hillslope processes (Tucker 1998), stream flow (Dingman 1978; Carlston 1966), flood peaks (Pallard et al. 2009; Ogden et al. 2011), mean annual discharge and sediment yields (Branson and Owen 1970; Wasson 1994; Binger et al. 1997; Biswas et al. 1999). It has also been used to detect variations of rock types and structure by photo-geologists to document the stage of erosional evolution of a drainage system and in land reclamation studies.

- **Drainage texture**: Postulated by Smith (1950), it is obtained by multiplying the stream frequency and drainage density parameters, and is indicative of the mesh of drainage lines that have developed over a surface. Thus indirectly, it also points towards the lithological, structural, pedological and climatic set up of an area. The scale of drainage texture after Pal (1972) is coarse (<4), intermediate (4–10), fine (10–50) and ultrafine (>50).

- **Ruggedness index**: It is a parameter used to describe how rugged the terrain is (Horton 1945), with terrain ruggedness being a feature of areas having high relief variations as a result of dissection sub-aerial denudational processes. The more dissected the topography, the more rugged it appears, being a combined expression of relief, texture and slope steepness.

## 6.3   Study Area

### 6.3.1   River Course and Basin Physiography

The Kharkai River flows due NNE (north north-east) and then NNW (north north-west) for a distance of 63 km from its source in the Bamanghati–Kolhan upland area through the Singhbhum plain, before the river takes a sharp turn due east within the Achaean terrain of southern Singhbhum that includes areas of Jharkhand and Odisha (Fig. 6.1). The Kharkai follows a roughly east north-east (ENE) course till it confluences with the Subarnarekha, its trunk stream, at Adityapur near Jamshedpur in Saraikela-Kharsawan district of Jharkhand (Fig. 6.1). The river basin covers approximately 6255.75 sq.km. and has a perimeter of about 774.05 km.

The Kharkai, with a width of 15 to 30 m, has a meandering course and a steep gradient for the first 40 km of its course and a relatively steeper gradient between the 350 and 225 m contours, situated mainly within the iron ore series of rocks. Part of the gentle gradient section is found in the NNW course and the rest is in the eastern course on either side of the abrupt right-angled turn in the Kharkai River beyond Chaibasa. The upper reaches are marked by meandering index (mean) of 1.3 with a mean gradient 1:30 and 1:350 for the southern and northern segments, respectively.

This Kharkai Basin mostly covers the south-western part of Subarnarekha basin, and geomorphologically it consists of a several distinct planation surfaces at varying altitudes (Fig. 6.2).
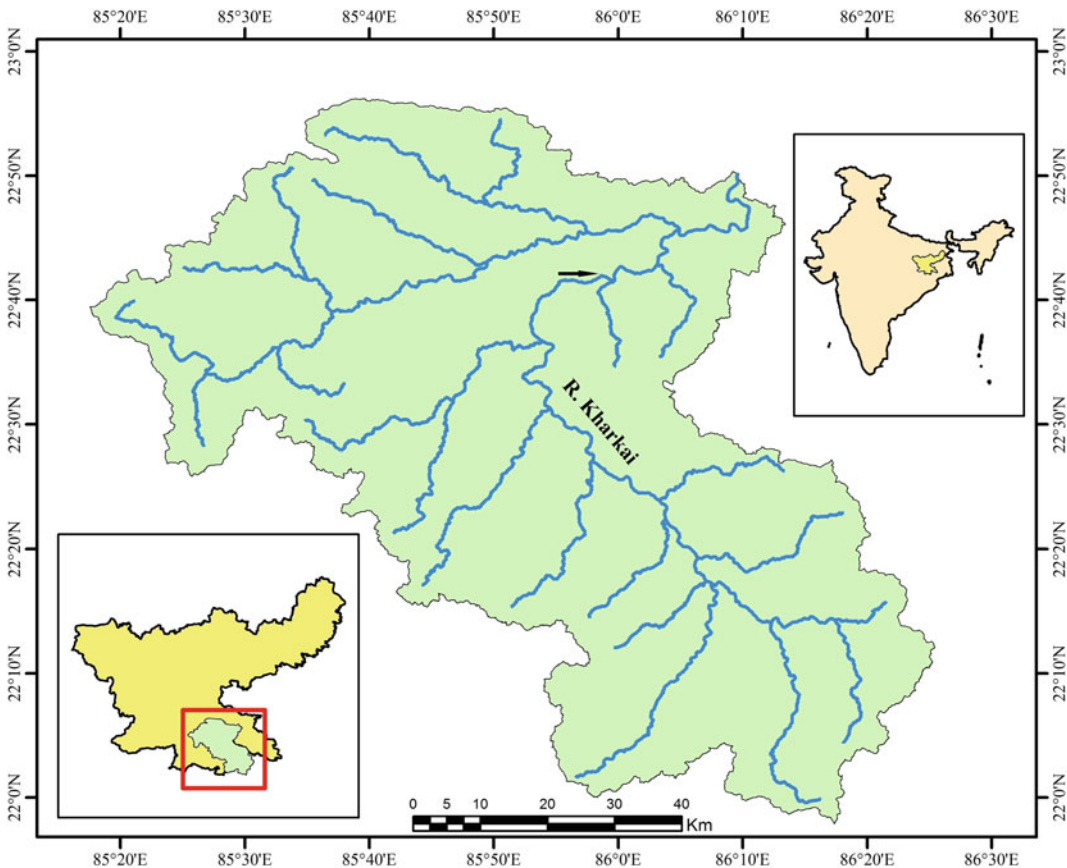


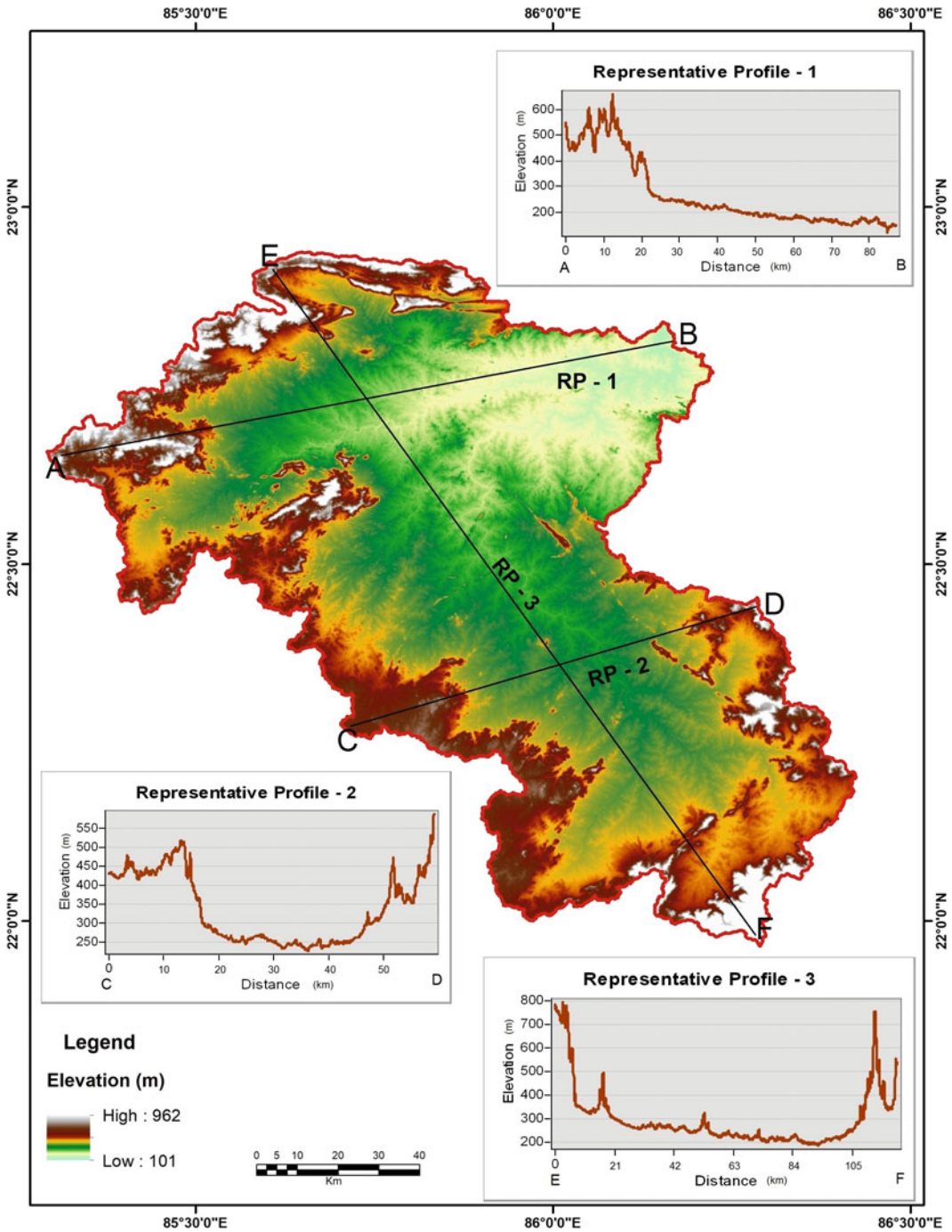**Fig. 6.1** Location of the Kharkai River Basin

**Fig. 6.2** Digital elevation model of the Kharkai River Basin, showing the elevation distribution and representative surface profiles with major planation surfaces

The elevation is between 960 and 130 m, respectively, with the altitude range being 830 m. The highest surface is along the southern rim built up by the Bamanghati–Kolhan upland and the northern Porahat hill formations. This rises to over 600 m. above sea level, within

which the river's meandering index varies from 1.2 to 1.38 and mean gradient is 1:30. This ridgeline actually forms the water divide in between the Koel (South), Baitarani and Subarnarekha drainage systems. The second surface within which the river has a meandering index from 1.2 to 1.38 and mean gradient less than 1:350, lies below an average altitude of 600 m. It is an extensive belt stretching in an irregular manner, thus fencing the basin in its north, west and southern part in a striking way. This planation surface rises to above 300 m and corresponds mostly to the iron ore series and Singhbhum granite formations (Mukhopadhyay 1980).

### 6.3.2   Climatic Attributes and Soil Cover

This river basin has a tropical monsoon climatic regime with alternate dry and wet seasons (Singh 1975). The hot weather commences in March and temperatures rise sharply till May, when the mean monthly temperature is between 29 and 32 °C. During the summer southwest monsoon (June–October), the rainfall received is between 100 and 150 cms, which is almost 90% of the total. Since, the Kharkai is seasonal, its discharge is highest during July–August, with a strongly leptokurtic hydrograph. January has the lowest temperatures (mean of around 16.4 °C).

The soil cover varies according to the parent rock and mostly contains high ferric oxide and bauxite, which tinges them red. A mixture of lateritic, black and red soils is predominantly found over the area. These soils range from laterite and lateritic soils on the high plateau surfaces in the north along Dalbhum and in the south around Simlipal (Singh 1975). Yellow grey loams and black and brown soils are found within valley floors or in predominantly lowland areas along the trunk stream of Kharkai and its major tributaries. The tertiary soils contain gravel and grit with high alluvial content at Adityapur where the Kharkai meets the Subarnarekha. Loams of reddish yellow variety are found here with marked lateritic formations due to intense leaching by pluvial events, which are eroded and reworked by the initial stream

orders that dissect the river basin. Admixture of kaolin, siliceous matter and potash makes the soils here wet and sticky, retaining moisture for a long time but which become hard and friable when dry.

### 6.3.3   Basin Lithology

The area is principally underlain by Precambrian igneous and metamorphic rocks (Fig. 6.3a). Some sedimentary rocks are found along the courses of the main channels and there are some laterite patches in the area. The majority of the exposed rocks are granitoids, which are often weathered and fractured and have gneissic banding. Besides these, amphibolite and metabasics intrusions occur within the granitoid mass. The basin also contains a great variety of sheared and foliated formations since it is situated along and close to some major shear zones and fault lines that have created great contortions in the surface topography, forming twisted linear ridges (Mahadevan 2002). The sedimentaries usually occupy higher elevations, overlying the basics and metamorphics below. The sheared rocks are of many varieties and show different stages of prograding metamorphism, with the presence of micas, phyllites, schists, migmatites and gneiss.

The entire basin area may broadly be divided into two broad geological provinces though even within these two major divisions, there are the occasional patches of rocks of a differing character (Fig. 6.3b). This first group comprises Achaeans of granite and gneiss and such meta-igneous rocks, in the central and southern part of the basin. The second group is an amalgamation of sheared, heavily contorted and foliated rocks belonging to the schist and phyllite group (centering around large formations of quartzites) that are cut and intruded into by many formations of amphiboles and pyroxenes in the northern to central portion of the basin. This group shows a wider variety of lithological variations than the first one that is largely uniform, except where intruded into by amphiboles and epidiorites in the extreme south, along linear narrow ridges. All formations are intruded by pegmatites and quartz veins in lineament swarms.
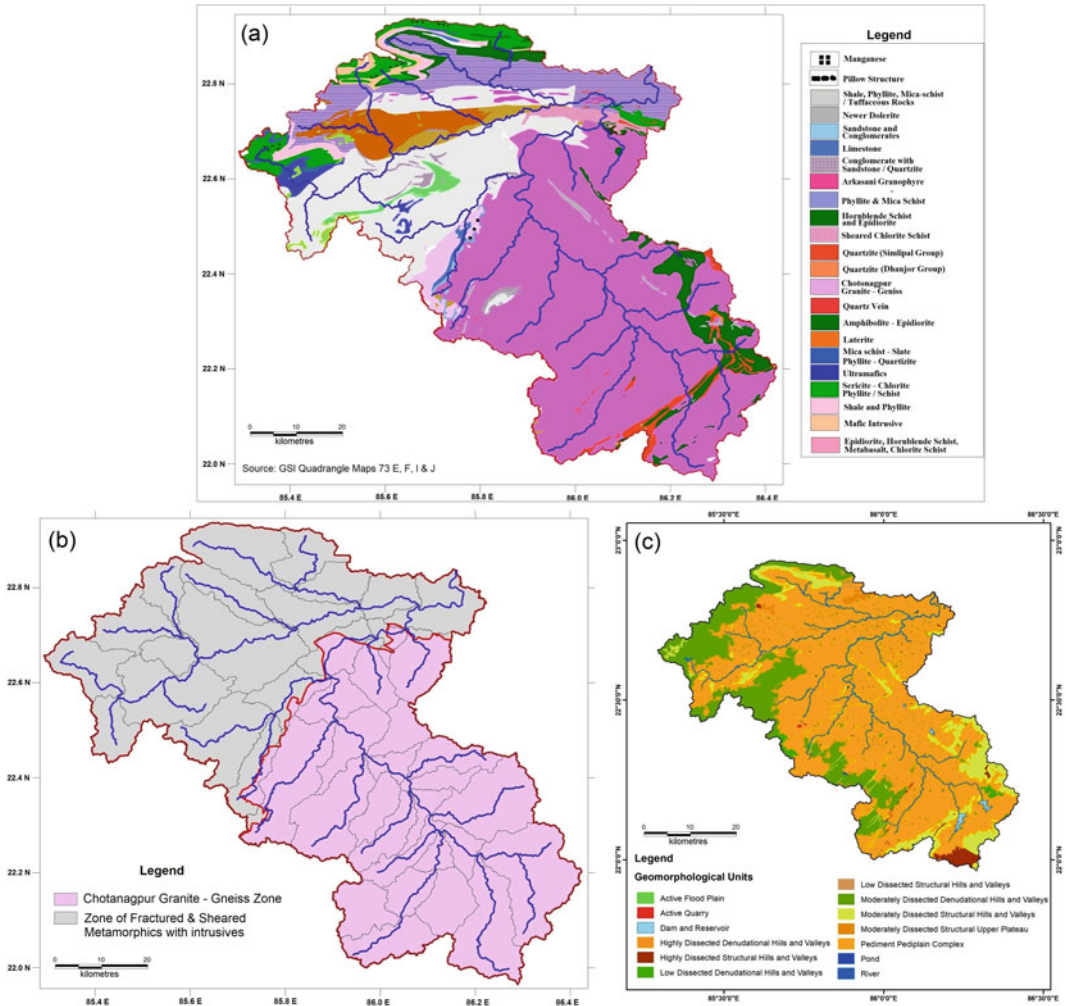
**Fig. 6.3** Landscape attributes- **a** Detailed lithological units, **b** Broad lithological groups, and **c** Geomorphological units

## 6.3.4 Basin Geomorphology

The plateau landscape is heavily eroded by the drainage network of the Kharkai and its major tributaries. The pediment-pediplain complex comprises almost 70% of the basin landscape (Fig. 6.3c). Next is the moderately dissected denudational hills and valleys along the edges of the river basin which account for 16.5% of the landscape while moderately dissected structural hills and valleys comprise the higher elevations and form 8.5% and are the source regions of most streams. Only 1% of the basin geomorphic constituents is comprised of highly dissected

structural hills and the smaller geomorphic units are very localized, contributing less than 1% of the landscape.

## 6.4 Results and Discussions

### 6.4.1 Enumerated Morphometric Parameters

Morphometric parameters consider variations in terrain attributes (shape/shape/alignment) and there are several parameters that reveal the varying aspects of the spatial geometry of the

**Table 6.2** Morphometric parameters used for terrain analysis of the Kharkai River Basin

| Parameter type | Morphometry base | Morphometric parameters | Enumeration | References |
|---|---|---|---|---|
| Terrain | Grid | Mean elevation | Average elevation of the river basin | |
| | | Relative relief | Maximum Elevation—Minimum Elevation | Smith (1935) |
| | | Average slope | $\tan^{-1}((N * CI)/636.6)$ (N = Average no. of contour crossings in each grid, CI = Contour Interval and 636.6 is a constant) | Wentworth (1930) |
| | | Dissection index | Relative Relief/Absolute Relief | Miller (1953) and Nir (1957) |
| | | Surrogate of hypsometry | (Mean Elevation—Minimum Elevation)/Relative Relief | Pike and Wilson (1971) |
| | Automated algorithm | Terrain surface texture | Spatial intricacy per unit area (i.e. drainage density and changes in sign of slope aspect or curvature) | Iwahashi and Pike (2007) |
| | | Terrain surface convexity | Segregation of high and low relief features | |
| | | Topographical wetness index | log [Flow Accumulation/tan (Slope in degree)] | Beven and Kirkby (1979) |
| | | Topographical position index | Measuring topographic slope positions and to automate landform classifications | Guisan et al. (1999) |
| Drainage | Grid | Stream frequency | No. of Stream segments flowing through a grid/Grid Area | Horton (1945) |
| | | Drainage density | Total Length of Streams of all order/Grid Area | |
| | | Drainage texture | Drainage Density $\times$ Stream Frequency | Smith (1950) |
| Terrain & drainage | | Ruggedness index | (Relative Relief $\times$ Drainage Density)/1000 | Horton (1945) |

landscape, each with their own benefits and weaknesses. The quantitative interpretation of the Kharkai River Basin using morphometric techniques provides a standardized scale of measurement and comparison of its various aspects. The statistical and graphical methods deal mainly with the relationship of the basin area to each surface attribute and their cartographical representation portrays the total character of the landscape. The type of morphometry, their method of extraction, individual formulae and description used to discuss each of them are presented in detail (Table 6.2).

The highest mean elevation zones are found along the extreme northern, north-western, south-eastern and eastern edges of the basin where it ranges between 750 and 800 m (Fig. 6.4a). The lowest values of 50−150 m abound around the confluence zone of the two major streams in the north-eastern section. Mostly, the mean elevation ranges between 150 and 200 m and comprises the entire central zone of the basin. Numerous

small streams dissect the higher elevation zones as they descend to the lower heights. The highest relative relief zones are observed along the northern, north-eastern, north-western, south-eastern and southern fringes of the river basin, ranging between 400 and 500 m, while rest of the basin is highly dissected by numerous small streams for which the relative relief is low, ranging between 50 and 150 m.

In the Kharkai River Basin, the highest average slope values are obviously found in the higher elevation zones, i.e. along the northern and southern periphery, with values between 24° and 30° (Fig. 6.4b). On the whole, the greatest part of the basin has slope values ranging between 6° and 12°. Almost the entire basin area is moderately dissected (values 0−0.2°) by the Kharkai, its main tributaries and numerous smaller streams, except a few more affected patches in the southern, northern and south-eastern fringes where values are around 0.5° −0.9°, due to the higher ambient slope and elevation (Fig. 6.5a). Higher HI values denote a greater volume of material still to be eroded from within that basin grid area while lower values point to more eroded tracts (Fig. 6.5b). Higher dissection has caused most of the basin landscape to have relatively lower HI values between 0.2 and 0.4, while higher values are present along the water divides to the south-west, south and north, where they are between 0.6 and 0.8. The higher HI values in a landscape that is otherwise geologically quite old are possible indicators of an ambient topographic disequilibrium (e.g. Guha and Patel 2017).

The terrain surface texture (TST) shows that the central portion of the basin, through which the major

rivers drain, have the least values, i.e. below 8, which means that the texture of the terrain surface is flat and therefore this corresponds to the pediplain-pediment complex (Fig. 6.6a). The foot slope areas of the dissected denudational hills are represented in lighter brown shades, with a value range of 8–16, and show a higher degree of texture roughness, while the highest range of > 32 is for the highland areas having remnants of few structural hills that are dissected by first order streams. The terrain surface convexity (TSC) map (Fig. 6.6b) shows that the higher elevation structural and denudational hills are having a clear convex slope with a value of more than 60, and stretching out till the foot slopes or pediments. Followed by this, the continuation of this value range of 40–60 clearly shows the undulating slopes of the pediment areas within the river basin of the Kharkai. Furthermore, the lowest range values of the below 20 group is the actual pediplan complex where the trunk streams of Kharkai and its major tributaries are continuously eroding the landscape in due achievement of gradation. The TWI map (Fig. 6.6c) shows that the Kharkai basin has negative values, i.e. below –10 in the higher elevation areas implying that these zones have higher runoff and least surface saturation. Contrastingly, the primary drainage area has higher values ranging from –1 to + 10, indicating how surface saturation along the stream courses increase and this rises to > 10 in those tracts that are adjacent to the central drainage network of the Kharkai and its tributaries.

In the Kharkai basin, the TPI values predominantly range between –5 and + 5, implying that the topography is mostly dissected by denudational process, i.e. the major streams
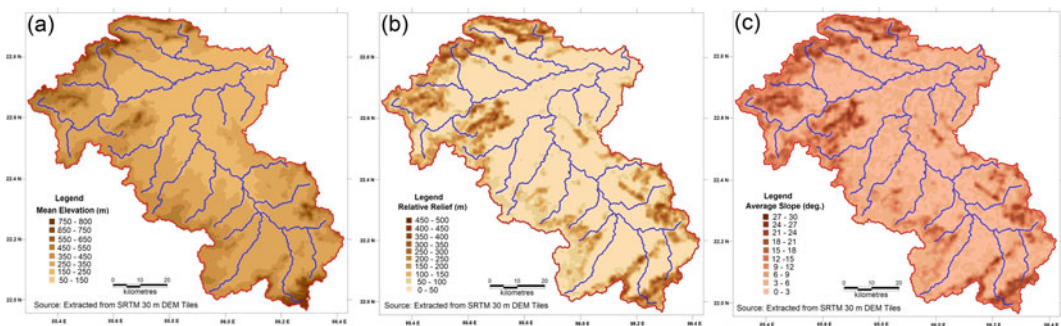


**Fig. 6.4** Traditional morphometric parameters (grid-based evaluation)- **a** Mean elevation, **b** Relative relief, and **c** Average slope
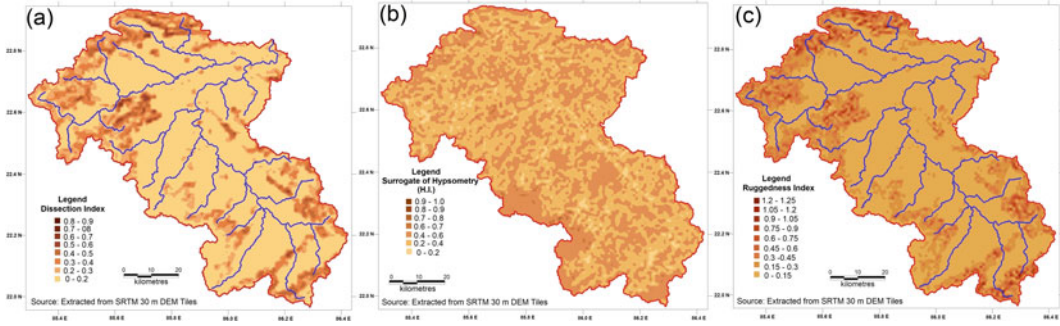
**Fig. 6.5** Traditional morphometric parameters (grid-based evaluation)- **a** Dissection Index, **b** Hypsometry, and **c** Ruggedness index
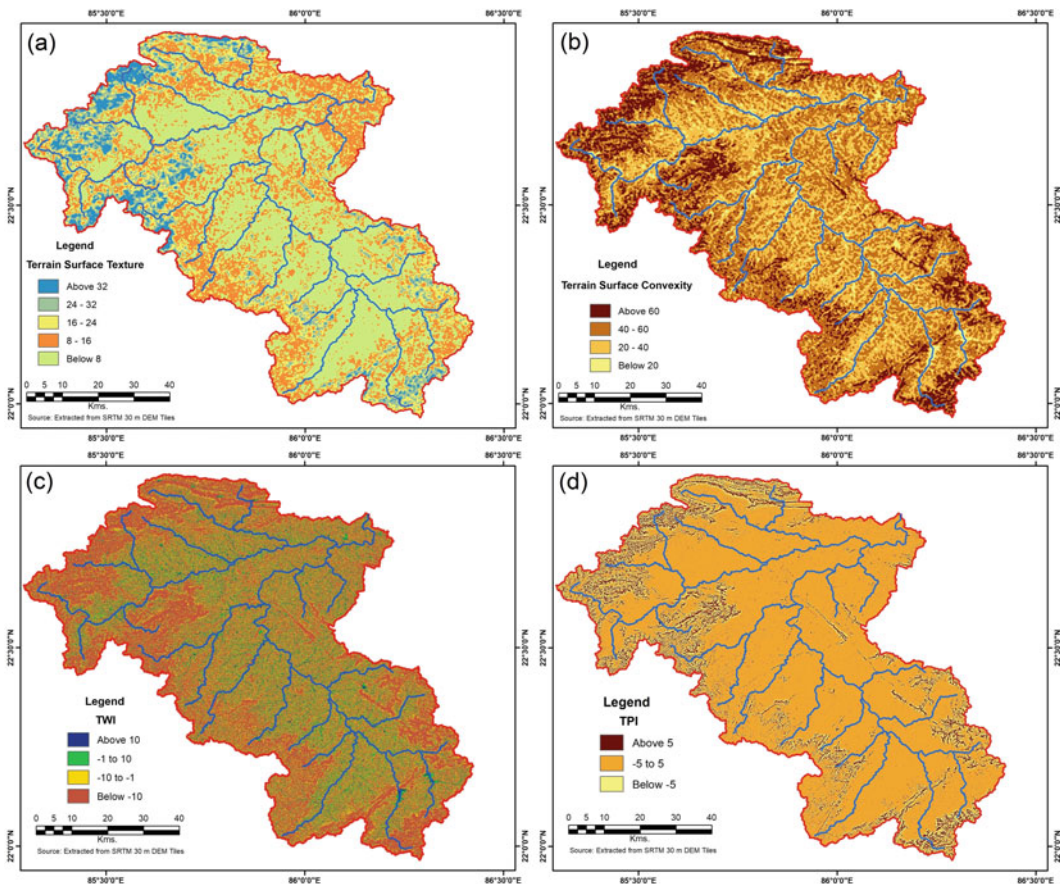


**Fig. 6.6** New topographic variables (DEM pixel-based evaluation)- **a** Terrain surface texture, **b** Terrain surface convexity, **c** Topographic wetness index, and **d** Topographic position index

(Fig. 6.6d). The higher altitude areas show values > 5, especially in the structural and denudational hill complex around the fringes of the river basin. Stream frequencies in the Kharkai basin range between 10 and 20 stream segments per sq. km. (Fig. 6.7a), except for some patches in the south-central, north-eastern and north-western parts, where the stream frequency is between
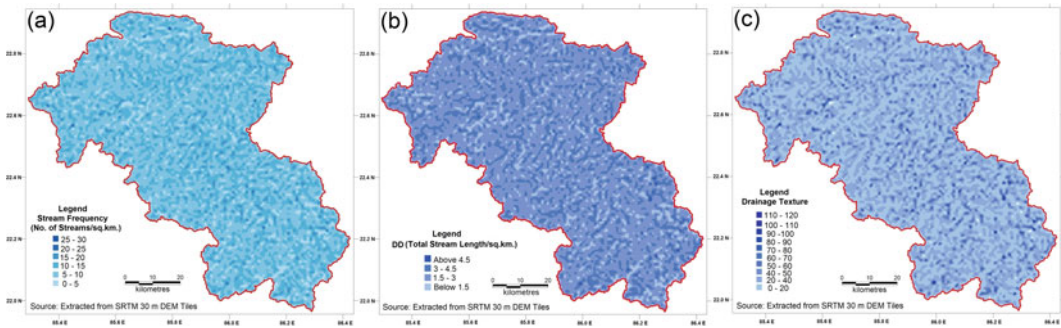
**Fig. 6.7** Drainage parameters- **a** Stream frequency, **b** Drainage density, and **c** Drainage texture

25 and 30, along the higher water divides that are drained by numerous smaller streams. The drainage density map of the Kharkai River basin (Fig. 6.7b) reveals that almost the entire area has a drainage density of 3.0 to 4.5 km/sq.km, with few patches ranging above 4.5 km/sq.km, along the principal confluence zones of the major trunk streams of the Kharkai and its tributaries. The drainage texture map (Fig. 6.7c) shows that drainage texture values lie between 40 and 70 for most of the basin, except some zones along the main stream course and its tributaries where values range between 90 and 120. Thus, the region mostly has an ultrafine drainage texture. Ruggedness index values in the central portion of the river basin range between 0.0 and 0.3 over the pediplain complex, with this being an uneven

plain or almost flat landscape drained by the major tributaries and the Kharkai itself (Fig. 6.5 c). The water divides exhibit greater ruggedness due to the presence of moderately dissected structural hills and valleys carved out by the numerous streams issuing forth therein.

## 6.4.2 Statistical Analysis of enumerated Morphometric Parameters

The different parameters computed above were arranged in the geo-database and their respective descriptive statistics were computed (Table 6.3). Their computed correlation coefficients

**Table 6.3** Descriptive statistics for the enumerated morphometric variables

| Measures | RR | AS | DI | RI | SF | DD | DT | HI |
|---|---|---|---|---|---|---|---|---|
| Mean | 73.70 | 5.89 | 0.17 | 0.14 | 8.61 | 2.30 | 23.32 | 0.38 |
| Median | 32.01 | 3.82 | 0.12 | 0.07 | 8.50 | 2.35 | 19.75 | 0.39 |
| Mode | 16.99 | 3.15 | 0.07 | 0.00 | 9.00 | 0.00 | 0.00 | 0.44 |
| Standard deviation | 78.51 | 4.92 | 0.12 | 0.16 | 4.12 | 1.03 | 17.86 | 0.11 |
| Sample variance | 6164.18 | 24.25 | 0.01 | 0.03 | 16.99 | 1.07 | 319.07 | 0.01 |
| Kurtosis | 2.19 | 1.57 | 0.30 | 6.39 | −0.06 | −0.31 | 1.23 | −0.16 |
| Skewness | 1.65 | 1.49 | 1.11 | 2.28 | 0.18 | −0.18 | 1.05 | −0.11 |
| Range | 439.01 | 28.11 | 0.61 | 1.30 | 29.00 | 5.43 | 118.28 | 0.71 |
| Minimum | 6.00 | 0.00 | 0.02 | 0.00 | 0.00 | 0.00 | 0.00 | 0.02 |
| Maximum | 445.01 | 28.11 | 0.63 | 1.30 | 29.00 | 5.43 | 118.28 | 0.73 |
| Count | 6616 | 6616 | 6616 | 6616 | 6616 | 6616 | 6616 | 6616 |

*Note* RR: Relative Relief; AS: Average Slope; DI: Dissection Index; RI: Ruggedness Index; SF: Stream Frequency; DD: Drainage Density; DT: Drainage Texture; HI: Hypsometric Integral

**Table 6.4** Correlation coefficients among the enumerated morphometric parameters

|      | RR    | AS    | DI    | RI    | SF    | DD    | DT    | HI   |
|------|-------|-------|-------|-------|-------|-------|-------|------|
| RR   | 1.00  |       |       |       |       |       |       |      |
| AS   | 0.86  | 1.00  |       |       |       |       |       |      |
| DI   | 0.93  | 0.83  | 1.00  |       |       |       |       |      |
| RI   | 0.72  | 0.76  | 0.73  | 1.00  |       |       |       |      |
| SF   | −0.29 | −0.14 | −0.27 | 0.15  | 1.00  |       |       |      |
| DD   | −0.33 | −0.17 | −0.30 | 0.20  | 0.83  | 1.00  |       |      |
| DT   | −0.28 | −0.18 | −0.27 | 0.14  | 0.93  | 0.90  | 1.00  |      |
| HI   | 0.05  | 0.03  | −0.09 | −0.22 | −0.35 | −0.40 | −0.37 | 1.00 |

*Note* RR: Relative Relief; AS: Average Slope; DI: Dissection Index; RI: Ruggedness Index; SF: Stream Frequency; DD: Drainage Density; DT: Drainage Texture; HI: Hypsometric Integral

(Table 6.4) reveal their interlinkages. Obviously, the topographic variables (RR, AS, DI and RI) and the drainage variables (SF, DD and DT) are strongly and positively correlated among themselves. Mostly, the drainage and topographic parameters are inversely related with each other, pointing to the paucity of drainage development in the higher elevations within the basin and the concentration of streamlines along the lower valley floors.

### 6.4.3 Factor Analysis and delineation of Morphometric Regions

While a correlation matrix states the relationship type between pairs of variables, factor analysis employs a 'factor loadings' matrix, that distinguishes the various 'basic' or 'abstract' variables, expressing the relationship level between these and the original variables and provides a simplified data matrix, i.e. the 'factor score' (or weightings) matrix. Beginning the analysis without any preconceived ideas as to the relative importance of the variables, it is initially reasonably presumed that each variable contributes the same amount of information to the study, and the lengths of the corresponding vectors are standardized. To ensure that all the vectors have the same origin, the mean of each variable is made equal to zero. Using such standardized vectors, the cosine of the angle separating any two vectors equals the coefficient of correlation between the corresponding variables.

Data reduction from the original eleven variables to a few significant factors was obtained by extracting and rotating the factor-loadings matrix, and the corresponding relationships were noted in terms of the percentage contributed to the variance of each variable by each rotated factor (Table 6.5). Four factors were significant, as they explained >80% of the total variation. The initial loadings on Factor-1 seemed to align closely with the variances. Factor One scores were thus mapped across the Kharkai Basin (Fig. 6.8) to derive regions which are the best representative amalgamation of the combinations of the different morphometric variables. The prepared maps show good visual correlation with the different terrain features and using this a number of terrain units were demarcated (Table 6.6). The proportion of basin area falling under each unit was also enumerated. It shows that the Kharkai Basin is mostly comprised of an undulating, at times broken, plain surface with local higher tracts. The unevenness of topographic classes is greater in the northern and western parts of the basin over the zone of fractured and sheared high grade metamorphics than over the Chota Nagpur granite-gneiss complex that forms the rest of the region. These maps of Factor One Scores describe the various types landforms developed from intensive and continuous riverine erosion. The central part of the basin has values between −2 and 0, indicative of gently sloping undulating plains. The northern fringes show summital convexities and some
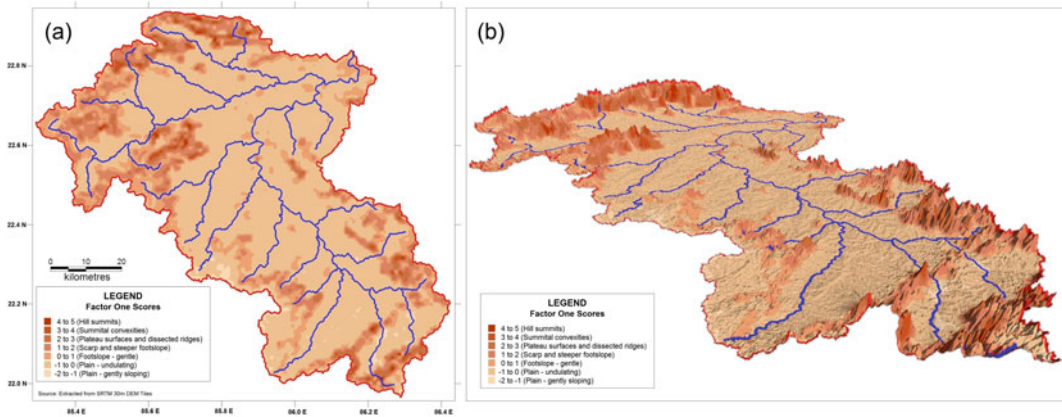
**Fig. 6.8** Factor One score-based landscape unit delineation in the Kharkai River Basin- **a** Planform view, and **b** 3-D perspective

hilly peaks, the north-western and west-central zones show dissected ridges and plateau surfaces with some intermittent heights. In the south, the range of topographic variation is from 0 to 3, i.e. mostly gentle foot slopes to dissected ridges and plateau surfaces.

### 6.4.4 Relating changing LULC attributes with the Terrain Units

Modification of the natural landscape by human activities leaves profound impacts and changing LULC patterns are a major component of many current ecological concerns, being recognized as key drivers of environmental change (Turner et al. 1993; Iqbal and Sajjad 2014). A comparative analysis of LULC units within the Kharkai basin was thus done to elicit the major changes within the Kharkai river basin from 1990 to 2020 (Fig. 6.9). There are six major LULC classes (Table 6.7), which are typically fragmented and conform to the usual types seen in the Chota Nagpur Plateau region (e.g. Chatterjee and Patel 2016; Sarkar and Patel 2016) and marked changes have occurred in each. Water bodies (which includes ponds and lakes) were seen to shrink with increasing prevalence of agriculture and forestry. Vegetation cover has depleted by over 246.99 km² and fallow land have declined by

243.44 km² from 1990 to 2020, with both of these contributing to more areal coverage under agriculture, which has seen a sharp rise of 494.38 km². Settlement coverage and those of mines and quarries have risen markedly during this time period, particularly the huge urban expansion of Jamshedpur and Adityapur, at the mouth of the river in the north-eastern part of the basin. While the rivers have also shown a minimal decline in its share of LULC units by 15.15 km², this may be due to image classification issues as well as from the continuous encroachment onto the river bed as a result of sand mining and farming on the principal stream and its tributaries.

The interrelations among the lithology, major geomorphic units, LULC with the factor-one score based topographic units and the automated algorithm-based geomorphometric parameters needs to be delved into further to understand the landscape fabric (Table 6.6). Higher TST values can be well related to the higher topographic classes discerned from factor one scores (like the hill summits and summital convexities) as the maximum and mean values express the high amount of ruggedness with greater values. The contrary is observed for the gentle undulating slopes in the pediment and pediplain complex, consisting of LULC units like agricultural lands, water bodies, settlements and fallow lands. The higher TSC values demarcating the hill tops and convex slopes of the moderately to highly

**Table 6.5** Explanation of total variance

| Component | Initial Eigen values | | | Extraction Sums of Squared Loadings | | | Rotation Sums of Squared Loadings | | |
|---|---|---|---|---|---|---|---|---|---|
| | Total | % of Variance | Cumulative % | Total | % of Variance | Cumulative % | Total | % of Variance | Cumulative % |
| 1 | 5.574 | 50.677 | 50.677 | 5.574 | 50.677 | 50.677 | 4.328 | 39.346 | 39.346 |
| 2 | 2.862 | 26.015 | 76.692 | 2.862 | 26.015 | 76.692 | 2.987 | 27.158 | 66.504 |
| 3 | 1.209 | 10.995 | 87.687 | 1.209 | 10.995 | 87.687 | 1.977 | 17.971 | 84.475 |
| 4 | 0.665 | 6.045 | 93.732 | 0.665 | 6.045 | 93.732 | 1.018 | 9.257 | 93.732 |
| 5 | 0.274 | 2.489 | 96.221 | | | | | | |
| 6 | 0.181 | 1.646 | 97.867 | | | | | | |
| 7 | 0.132 | 1.196 | 99.063 | | | | | | |
| 8 | 0.055 | 0.503 | 99.566 | | | | | | |
| 9 | 0.034 | 0.307 | 99.873 | | | | | | |
| 10 | 0.012 | 0.108 | 99.982 | | | | | | |
| 11 | 0.002 | 0.018 | 100 | | | | | | |

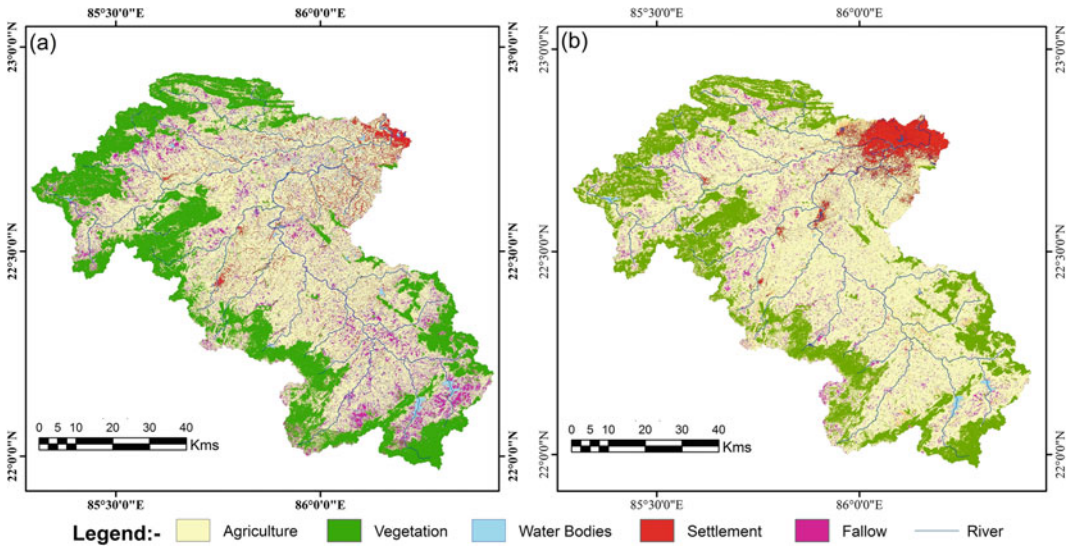Extraction Method: Principal Component Analysis with Varimax Rotation using Kaiser Normalization

**Fig. 6.9** LULC attributes in the Kharkai River Basin for the years- **a** 1990, and **b** 2020

dissected denudational hills and valleys predominantly have natural vegetation cover (forests). The other extreme of the TSC value range shows that lower mean values represent gentle or undulating slopes of the pediplain complex where the convexity is almost nil or near to zero. In case of TWI values, higher elevation areas from hill top summits to footslopes, highlight tracts where the amount of runoff is higher. The pediplain zone having the major rivers, settlements and agricultural lands are represented by low TWI scores and are underlain either by the Chota Nagpur gneiss-granite complex or the fractured and sheared metamorphic lithology that contains major intrusions. Lastly, the TPI values indicate the position of the topographic classes and is one of the best parameters to validate the morphometric regions derived based on the factor one scores. Extremely low TWI scores represent the central section of the river basin that is drained by major streams and is therefore ideal for practicing agriculture due to presence of major water bodies and available fallow land cover in the pediplain complex. The higher TWI

values corroborate quite perfectly with the factor one scores in showing higher elevations (scarplands, summital convexities and the hill summits majorly) that are moderate to highly dissected.

As is obvious, the nature of the terrain has an influence on the kind of landscape modification undertaken within the basin and the different terrain units demarcated on the basis of the morphometric attributes. Such modifications of the ambient geomorphic diversity of the Chota Nagpur region and its adjoining tracts through anthropogenic activities are quite common (Patel and Mondal 2019; Patel et al. 2020), while this also has a marked impact on the streamside ecology and degree of riparian naturalness and vegetation cover (Saha et al. 2020) along the principal river corridors (cf. Banerji and Patel 2019). The smaller hills and ridges and hill summits have been largely levelled in a series of broad terraces to enable cultivation (Fig. 6.10a) while the higher dissected plateau tracts have undergone marked clearing in their original vegetation cover (Fig. 6.10b). In the piedmont-pediplain zone and the footslopes of the ridges,

**Table 6.6** Different topographic classes or morphometric regions delineated using Factor One scores

| Factor score one range | Topographic class | Area (sq.km) | Proportion of Basin Area (%) | Main lithological attributes | Major landform assemblages | Dominant LULC Class | Terrain Surface Texture | | | Terrain Surface Convexity | | | Topographical Wetness Index | | | Topographical Position Index | | |
|---|---|---|---|---|---|---|---|---|---|---|---|---|---|---|---|---|---|---|
| | | | | | | | Max | Min | Mean | Max | Min | Mean | Max | Min | Mean | Max | Min | Mean |
| −2 to −1 | Plain—gently sloping, almost level | 92.09 | 1.47 | Chotanagpur granite-gneiss and fractured and sheared metamorphics with intrusives | Pediplain complex and active floodplain | Agriculture, water bodies, rivers, settlements and fallow land | 29.37 | 0.00 | 4.63 | 55.43 | 0.00 | 36.46 | 6.54 | −18.52 | −13.62 | 3.98 | −3.06 | 0.01 |
| −1 to 0 | Plain—undulating and dissected | 4100.28 | 65.35 | Chotanagpur granite-gneiss, fractured and sheared metamorphics, mafic intrusives, laterite and conglomerate/quartzite | Pediplain complex | Agriculture, water bodies, rivers, settlements and fallow land | 32.79 | 0.00 | 3.85 | 60.49 | 0.00 | 37.31 | 13.52 | −19.59 | −13.53 | 7.44 | −5.36 | −0.00 |
| 0 to 1 | Footslope—gentle | 1073.10 | 17.10 | Chotanagpur granite-gneiss, phyllite, mica schist and fractured and sheared metamorphics with intrusives | Pediment-pediplain complex | Agriculture, settlements and rivers | 37.10 | 0.17 | 10.88 | 61.43 | 1.9405 | 41.41 | 10.11 | −19.63 | −15.20 | 10.53 | −6.72 | −0.03 |
| 1 to 2 | Scarp and steeper footslope | 674.58 | 10.75 | Chotanagpur granite-gneiss, hornblende, schist and epidiorite and ultramafic instrusives | Pediment complex and low dissected structural/denudational hills | Vegetation cover and rivers | 40.17 | 0.41 | 15.05 | 63.15 | 8.791 | 43.60 | 8.88 | −20.04 | −16.04 | 11.93 | −7.58 | −0.00 |
| 2 to 3 | Plateau surfaces and dissected ridges | 259.65 | 4.14 | Chotanagpur granite-gneiss, amphibolite-epidiorite and limestone | Moderate to low dissected denudational/ structural hills and valleys | Vegetation cover and rivers | 37.30 | 1.16 | 15.98 | 65.09 | 10.072 | 45.25 | 4.55 | −20.48 | −16.43 | 15.95 | −9.75 | 0.04 |
| 3 to 4 | Summital convexities | 66.53 | 1.06 | Chotanagpur granite-gneiss, amphibolite-epidiorite, serite-chlorite, phyllite/ schist and fractured and sheared metamorphics with intrusives | Moderate to low dissected denudational/ structural hills and valleys | Vegetation cover | 35.81 | 2.56 | 16.06 | 63.92 | 27.582 | 46.20 | 6.33 | −20.49 | −16.57 | 11.90 | −15.86 | 0.07 |
| 4 to 5 | Hill summits | 7.71 | 0.12 | Chotanagpur granite-gneiss, amphibolite-epidiorite and fractured and sheared metamorphics with intrusives | High to Moderate dissected denudational/ structural hills | Vegetation cover | 32.59 | 2.17 | 15.15 | 63.74 | 27.992 | 46.05 | 0.80 | −20.82 | −16.71 | 14.20 | −11.70 | −0.01 |

**Table 6.7** Changes in LULC observed within the Kharkai River Basin from 1990 to 2020

| Sl. no | LULC class | Years | | Change matrix 2020 −1990 | Interpretation |
|---|---|---|---|---|---|
| | | 2020 | 1990 | | |
| | | Area (sq. km.) | | | |
| 1 | Water bodies | 18.61 | 60.31 | −41.70 | Major shrinkage and drying up of water bodies |
| 2 | Vegetation | 1547.62 | 1794.61 | −246.99 | Depletion of vegetation cover |
| 3 | River | 97.44 | 112.59 | −15.15 | Decrease of riverine drainage due to drying up of streams and encroachment of river beds for agriculture |
| 4 | Settlement | 357.79 | 304.89 | +52.90 | Massive urban expansion—Jamshedpur and Adityapur |
| 5 | Fallow | 254.37 | 497.81 | −243.44 | Major decline in fallow land coverage |
| 6 | Agriculture | 3979.92 | 3485.54 | +494.38 | Major rise of area under agriculture |
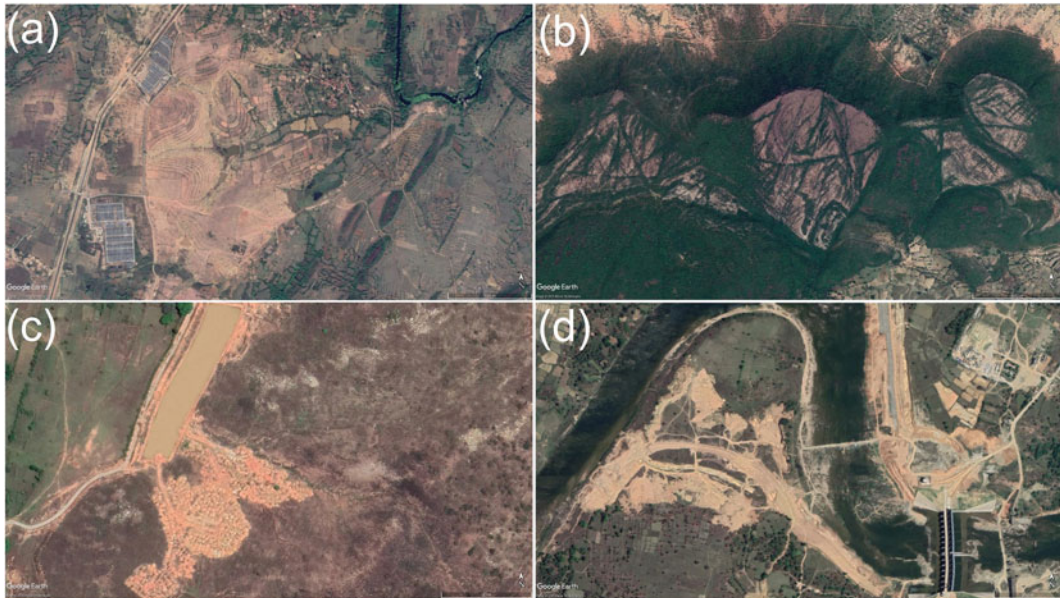


**Fig. 6.10** Google Earth screenshots of LULC changes in the Kharkai Basin- **a** Planation and deforestation of the small hills for agriculture, **b** Deforestation occurring in plateau surface and dissected ridges, **c** Hollowing of pediplain-piedmont and foot slope areas for local water harvesting, and **d** Excavations along gently undulating surfaces and floodplains for irrigation and transport infrastructure. *Note* All images are aligned to north vertically upwards

local surface water harvesting measures have formed landforms of excavation and accumulation (Szabo 2006), with ponds dug up and mounds of earth piled around (Fig. 6.10c). Along the gently sloping floodplains and undulating surfaces by the major stream courses, more extensive earth-moving measures have ensued to create transport and irrigation facilities (Fig. 6.10d). Further assessment of the soil loss occurring from the basin as a result of these LULC changes can be discerned by using methods like the Universal Soil Loss Equation (Majhi et al. 2021). Further assessment of the soil loss occurring from the basin as a result of these LULC changes can be discerned by using methods like the Universal Soil Loss Equation (Majhi et al. 2021).

## 6.5   Conclusion

Landscape characterization has been performed in this study to develop an understanding about how different geomorphometric parameters are derived based on conventional grid system and from recently developed automated algorithms in a geospatial environment. The central section of the Kharkai River basin was found to be heavily eroded by the principal tributaries and by the Kharkai itself, while the edges of the river basin are composed of high to moderately dissected denudational ridges and some structural hills and valleys. The various morphometric parameters were statistically correlated with each another to delineate distinct terrain units using PCA. Strong positive correlations were obtained among the drainage and topographic variables while inverse relations were elicited between the drainage and topographic parameters. An abundance of drainage development in the higher elevations and clustering of major tributaries along the lower valley floors was discerned. The correlation matrix was further used to develop major physiographic zones using factor one scores to decipher the most pertinent topographic classes to describe the landscape of this river catchment. Two major lithological formations, i.e. the Chota

Nagpur granite-gneiss complex in the south and the fractured and sheared metamorphics containing intrusives in the northern half of the river basin were corroborated with the present-day LULC units. The respective areal coverage under settlements and agriculture has seen a major rise in the past thirty years while there has been a considerable decline in the natural vegetation cover (forests), fallow land and water bodies. Some evidences from Google Earth imagery were collected across the basin to showcase the major alterations occurring under the various topographic classes. The need for planning and implementation of land and water conservation schemes can hence be practiced for the most anthropogenically modified and erodible portions to protect the landscape from further degradation.

## References

Agarwal CS (1998) Study of drainage pattern through aerial data in Naugarh area of Varanasi district, U. P. J Indian Soc Rein Sens 24(4):169–175

Altaf S, Meraj G, Romshoo SA (2014) Morphometry and land cover based multi-criteria analysis for assessing the soil erosion susceptibility of the western Himalayan watershed. Environ Monit Assess 186 (12):8391–8412

Aparna P, Nigee K, Shimna P, Drissia TK (2015) Quantitative analysis of geomorphology and flow pattern analysis of Muvattupuzha River basin using geographic information system. J Aquatic Procedia 4:609–616

Asfaw D, Workineh G (2019) Quantitative analysis of morphometry on Ribb and Gumara watersheds: Implications for soil and water conservation. Int Soil Water Conserv Res 7(2):150–157. https://doi.org/10.1016/j.iswcr.2019.02.003i

Ayalew L, Yamagishi H (2004) Slope failures in the Blue Nile basin, as seen from landscape evolution perspective. Geomorphology 57:95–116

Banerji D, Patel PP (2019) Morphological aspects of the bakreshwar river corridor, West Bengal, India. In: Das B, Ghosh S, Islam A (eds) Advances in micro geomorphology of lower ganga basin - Part I: fluvial geomorphology, Springer International Publishing, Cham, pp 155–189. https://doi.org/10.1007/978-3-319-90427-6_9

Barling RD, Moore ID, Grayson RB (1994) A quasi-dynamic wetness index for characterizing the spatial distribution of zones of surface saturation and soil water content. Water Resour Res 30:1029–1044

Beven KJ, Kirkby MJ (1979) A physically based, variable contributing area model of basin hydrology/Un modèle à base physique de zone d'appel variable de l'hydrologie du bassin versant. Hydrol Sci J 24(1):43–69

Bingner RL, Garbrecht J, Arnold JG, Srinivasan R (1997) Effect of watershed subdivision on simulation runoff and fine sediment yield. Transact ASAE 40(5):1329–1335

Biswas S, Sudhakar S, Desai VR (1999) Prioritisation of sub watersheds based on morphometric analysis of drainage basin: a remote sensing and GIS approach. J Indian Soc Remote Sens 27(3):155

Branson FA, Owen JB (1970) Plant cover, runoff, and sediment yield relationships on Mancos Shale in western Colorado. Water Resour Res 6(3):783–790

Burrough PA, McDonnell RA (1998) Principles of geographical information systems. Oxford University Press Inc., New York

Carlston CW (1966) The effect of climate on drainage density and streamflow. Hydrol Sci J 11(3):62–69. https://doi.org/10.1080/02626666609493481

Chatterjee S, Patel PP (2016) Quantifying landscape structure and ecological risk analysis in Subarnarekha sub-watershed, Ranchi. In: Mondol DK (ed) Application of geospatial technology for sustainable development. University of North Bengal, India, North Bengal University Press, Raja Rammohunpur, pp 54–76

Chattopadhyay S, Carpenter RA (1990) A theoretical framework for sustainable development planning in the context of a river Basin. Unpublished Report, East-West Centre, Hawaii, 327–335

Chorley RJ, Schumm SA, Sugden DE (1984) Geomorphology. Methuen, London

Clarke JI (1996) Morphometry from Maps. Essays in geomorphology, Elsevier Publications, New York, 235–274

Cox RT (1994) Analysis of drainage-basin symmetry as a rapid technique to identify areas of possible quaternary tilt-block tectonics: an example from the Mississippi embayment. Geol Soc Am Bull 106:571–581

Das S, Pardeshi SD, Kulkarni PP, Doke A (2018) Extraction of lineaments from different azimuth angles using geospatial techniques: a case study of Pravara basin, Maharashtra, India. Arab J Geosci 11(8):160. https://doi.org/10.1007/s12517-018-3522-6

Das S, Pardeshi SD (2018) Morphometric analysis of Vaitarna and Ulhas river basins, Maharashtra, India: using geospatial techniques. Appl Water Sci 8(6):158. https://doi.org/10.1007/s13201-018-0801-z

Das S, Patel PP, Sengupta S (2016) Evaluation of different digital elevation models for analyzing drainage morphometric parameters in a mountainous terrain: a case study of the Supin—upper tons Basin, Indian Himalayas. SpringerPlus 5(1544). DOI: https://doi.org/10.1186/s40064-016-3207-0

De Martonne E (1934) Problemes Morphologiques du Bresil Tropical Atlantique. Annales De Geographie. 49:16–27

De Reu J, Bourgeois J, Bats M, Zwertvaegher A, Gelorini V, De Smedt P, ... Van Meirvenne M (2013) Application of the topographic position index to heterogeneous landscapes. Geomorphology 186:39–49. https://doi.org/10.1016/j.geomorph.2012.12.015

Deumlich D, Schmidt R, Sommer M (2010) A multiscale soil–landform relationship in the glacial-drift area based on digital terrain analysis and soil attributes. J Plant Nutr Soil Sci 173:843–851

Dingman SL (1978) Drainage density and streamflow: a closer look. Water Resour Res 14(6):1183–1187

Evans IS (1972) General geomorphometry, derivatives of altitude, and descriptive statistics. In Chorley RJ (ed) Spatial analysis in geomorphology. Harper and Row, New York, pp. 17–90

Evans IS (1984) Correlation structures and factor analysis in the investigation of data dimensionality: statistical properties of the Wessex land surface, England. In Proceedings of the Int. Symposium on Spatial Data Handling, Zurich., v 1. Geographisches Institut, Universitat Zurich-Irchel. pp 98–116

Francés AP, Lubczynski MW (2011) Topsoil thickness prediction at the catchment scale by integration of invasive sampling, surface geophysics, remote sensing and statistical modeling. J Hydrol 405:31–47

Gallant JC, Wilson JP (2000) Primary topographic attributes. In: Wilson JP, Gallant JC (eds) Terrain analysis: principles and applications. Wiley, New York, pp 51–85

Ghosh KG (2016) Spatial heterogeneity of catchment morphology and channel responses: a study of Bakreshwar River Basin, West Bengal. J Ind Geomorphol 4:47–64

Gizachew K, Berhan G (2018) Hydro-geomorphological characterization of Dhidhessa River Basin, Ethiopia. Int Soil Water Conserv Res 6:175–183. https://doi.org/10.1016/j.iswcr.2018.02.003

Goodbred SL Jr (2003) Response of the Ganges dispersal system to climate change: a source-to-sink view science the last interstade. Sediment Geol 162:83–104. https://doi.org/10.1016/S0037-0738(03)00217-3

Grohmann CH, Riccomini C (2009) Comparison of roving-window and search-window techniques for

characterising landscape morphometry. Comput Geosci 35:2164–2169

Guha S, Patel PP (2017) Evidence of topographic disequilibrium in the Subarnarekha River Basin, India: a digital elevation model based analysis. J Earth Syst Sci 126:106. https://doi.org/10.1007/s12040-017-0884-1

Guisan A, Weiss SB, Weiss AD (1999) GLM versus CCA spatial modeling of plant species distribution. Plant Ecol 143:107–122

Gutema D, Kassa T, Sifan A, Koriche (2017) Morphometric analysis to identify erosion prone areas on the upper blue Nile using GIS: case study of Didessa and Jema sub-basin, Ethiopia. Intern Res J Eng Technol 04 (08)

Guth PL (2001) Quantifying terrain fabric in digital elevation models. Environ Legacy Military Operat Geol Soc Am Rev Eng Geol 14:13–25

Hammond EH (1954) A geomorphic study of the Cape Region of Baja California (Vol. 10). University of California Press

Harinath V, Raghu V (2013) Morphometric analysis using Arc GIS techniques a case study of Dharurvagu, south eastern part of Kurnool district, Andhra Pradesh, India. Int J Sci Res 2(1):2319–7064

Horton RE (1932) Drainage basin characteristics. EOS Trans Am Geophys Union 13(1):350–361

Horton RE (1945) Erosional development of streams and their drainage basins; hydrophysical approach to quantitative morphology. Geol Soc Am Bull 56 (3):275–370

Hurtrez JE, Sol C, Lucazeau F (1999) Effect of drainage area on hypsometry from an analysis of small-scale drainage basins in the Siwalik hills (central Nepal). Earth Surf Process Landform 24:799–808

Illés G, Kovács G, Heil B (2011) Comparing and evaluating digital soil mapping methods in a Hungarian forest reserve. Can J Soil Sci 91:615–626

Iqbal M, Sajjad H (2014) Watershed prioritization using morphometric and land use/land cover parameters of Dudhganga Catchment Kashmir Valley India using spatial technology. J Geophy Remote Sens 3:12–23. https://doi:https://doi.org/10.4172/2169-0049.1000115

Islam A, Barman SD (2020) Drainage basin morphometry and evaluating its role on flood-inducing capacity of tributary basins of Mayurakshi River. India. https://doi.org/10.1007/s42452-020-2839-4

Iwahashi J, Pike RJ (2007) Automated classifications of topography from DEMs by an unsupervised nested-means algorithm and a three-part geometric signature. Geomorphology 86:409–440

Iwahashi J (1994) Development of landform classification using the digital elevation model. Ann Disaster Prev Res Inst, Kyoto Univ 37(B-1):141–156 (in Japanese with English abstract and illustrations)

Iwahashi J, Kamiya I (1995) Landform classification using digital elevation model by the skills of image processing—mainly using the Digital National Land Information. Geoinformatics 6(2):97–108 (in Japanese with English abstract)

Iwahashi J, Watanabe S, Furuya T (2001) Landform analysis of slope movements using DEM in Higashikubiki area. Japan. Comput. Geotech. 27:851–865

Javed A, Khanday MY, Ahmed R (2009) Prioritization of sub-watersheds based on morphometric and land use analysis using remote sensing and GIS techniques. J Indian Soc Remote Sens 37(2):261. https://doi.org/10.1007/s12594-009-0079-8

Javed A, Khanday MY, Rais S (2011) Watershed prioritization using morphometric and land use/land cover parameters: a remote sensing and GIS based approach. J Geol Soc India 78(1):63. https://doi.org/10.1007/s12594-011-0068-6

Jensen SK (1991) Applications of hydrologic information automatically extracted from digital elevation models. Hydrol Proc 5(1):31–44

Kabite G, Gessesse B (2018) Hydro-geomorphological characterization of Dhidhessa River basin, Ethiopia. Int Soil Water Conser Res 6(2):175–183. https://doi.org/10.1016/j.iswcr.2018.02.003

Khare D, Mondal A, Mishra PK, Kundu S, Meena PK (2014) Morphometric analysis for prioritization using remote sensing and GIS techniques in a Hilly catchment in the state of Uttarakhand, India. Indian J Sci Technol 7(10):1650–1662

Krishnamurthy J, Srinivas G, Jayaraman V, Chandrasekhar MG (1996) Influence of rock types and structures in the development of drainage networks in typical hardrock terrain. ITC J 3–4:252–259

Kumar A, Pandey RN (1982) Quantitative Analysis of Relief of the Hazaribagh Plateau Region. Perspect Geomorphol 1:235

Kumar R, Kumar S, Lohani AK, Nema RK, Singh RD (2000) Evaluation of geomorphological characteristics of a catchment using GIS. Gis India 9(3):13–17

Langbein WB, Leopold LB (1964) Quasi-equilibrium states in channel morphology. Am J Sci 262(6):782–794

Leopold LB, Wolman MG, Miller JP (1995) Fluvial processes in geomorphology. Courier Corporation

Lesschen JP, Kok K, Verburg PH, Cammeraat LH (2007) Identification of vulnerable areas for gully erosion under different scenarios of land abandonment in southeast Spain. CATENA 71:110–121

Lin Z, Oguchi T (2004) Drainage density, slope angle, and relative basin position in Japanese bare lands from high-resolution DEMs. Geomorphology 63(3–4):159–173

Liu H, Bu R, Liu J, Leng W, Hu Y, Yang L, Liu H (2011) Predicting the wetland distributions under climate warming in the Great Xing'an Mountains, northeastern China. Ecol Res 26:605–613

Liu M, Hu Y, Chang Y, He X, Zhang W (2009) Land use and land cover change analysis and prediction in the upper reaches of the Minjiang River, China. Environ Manage 43:899–907

Mahadevan TM (2002) Text book series 14: Geology of Bihar and Jharkhand; Geol. Soc. India, Bangalore

Majhi A, Shaw R, Mallick K, Patel PP (2021) Towards improved USLE-based soil erosion modelling in India: a review of prevalent pitfalls and implementation of exemplar methods. Earth-Sci Rev 221:103786. https://doi.org/10.1016/j.earscirev.2021.103786

Maune DF (2001) Digital elevation model technologies and applications: the DEM user's manual (Bethesda, MD: American Society for Photogrammetry and Remote Sensing)

McGarigal K, Tagil S, Cushman S (2009) Surface metrics: an alternative to patch metrics for the quantification of landscape structure. Landscape Ecol 24:433–450

Merritts D, Vincent KR (1989) Geomorphic response of coastal streams to low, intermediate, and high rates of uplift, Mendocino junction region, northern California. Geol Soc Am Bull 101:1373–1388

Miller VC (1953) Quantitative geomorphic study of drainage basin characteristics in the Clinch Mountain area, Virginia and Tennessee. Technical report (Columbia University. Department of Geology); no. 3, 189–200

Moglen GE, Eltahir EA, Bras RL (1998) On the sensitivity of drainage density to climate change. Water Resour Res 34(4):855–862

Mora-Vallejo A, Claessens L, Stoorvogel J, Heuvelink GBM (2008) Small scale digital soil mapping in southeastern Kenya. CATENA 76:44–53

Morisawa ME (1959) Relation of morphometric properties to runoff in the Little Mill Creek. Department of Geology-Columbia University, Ohio

Mueller JE (1968) An introduction to the hydraulic and topographic sinuosity indexes. Ann Assoc Am Geogr 58(2):371–385

Mukhopadhyay SC (1980) Geomorphology of the Subarnarekha Basin: the Chota Nagpur Plateau. University of Burdwan, Eastern India

Nag SK, Chakraborty S (2003) Influence of rock types and structures in the development of drainage network in hard rock area. J Indian Soc Remote Sens 31(1):25–35

Nir D (1957) Maps of dissection index of terrain. Proceedings of the Yorkshire Geological Society, 29

Obi Reddy GP, Maji AK, Gajbhiye KS (2004) Drainage morphometry and its influence on landform characteristics in a basaltic terrain, Central India–a remote sensing and GIS approach. Int J Appl Earth Obs Geoinf 6(1):1–16

Obi Reddy GE, Maji AK, Gajbhiye KS (2002) GIS for morphometric analysis of drainage basins. GisIndia 11 (4):9–14

Ogden FL, Raj Pradhan N, Downer CW, Zahner JA (2011) Relative importance of impervious area, drainage density, width function, and subsurface storm drainage on flood runoff from an urbanized catchment. Water Res Res **47**(12)

Oguchi T (1997) Drainage density and relative relief in humid steep mountains with frequent slope failure. Earth Surface Proc Landforms J British Geomorphol Group 22(2):107–120

Ohmori H (1993) Changes in the hypsometric curve through mountain building resulting from concurrent tectonics and denudation. Geomorphology 8:263–277

O'Loughlin EM (1986) Prediction of surface saturation zones in natural catchments by topographic analysis. Water Resour Res 22(5):794–804

Pal SK (1972) A classification of morphometric methods of analysis: an appraisal. Geog Rev India 34(1):61–84

Pallard B, Castellarin A, Montanari A (2009) A look at the links between drainage density and flood statistics. Hydrol Earth Syst Sci 13(7):1019

Patel A, Katiyar KS, Prasad V (2016) Performances evaluation of different open source DEM using Differential Global positioning system (DGPS). Egyptian J Remote Sens Space Sci 19(1):7–16

Patel PP (2012) An exploratory geomorphological analysis using modern techniques for sustainable development of the Dulung river basin. Unpublished PhD Thesis, University of Calcutta, Kolkata. https://shodhganga.inflibnet.ac.in/handle/10603/156681

Patel PP (2013) GIS techniques for landscape analysis—case study of the Chel River Basin, West Bengal. Proceedings of State Level Seminar on Geographical Methods in the Appraisal of Landscape, held at Dept. of Geography, Dum Dum Motijheel Mahavidyalaya, Kolkata, on 20th March, 2012, pp 1–14.

Patel PP, Sarkar A (2009) Application of SRTM data in evaluating the morphometric attributes: a case study of the Dulung River Basin. Pract Geograp 13(2):249–265

Patel PP, Sarkar A (2010) Terrain characterization using SRTM data. J Indian Soc Remote Sens 38(1):11–24. DOI: https://doi.org/10.1007/s12524-010-0008-8

Patel PP, Mondal S (2019) Terrain—landuse relation in garbeta-I block, paschim medinipur district, West Bengal. In: Mukherjee S (ed) Importance and Utilities of GIS, Avenel Press, Burdwan, pp 82–101

Patel PP, Mondal S, Prasad R (2020) Modifications of the geomorphic diversity by anthropogenic interventions in the silabati river basin. In: Das BC, Ghosh S, Islam A, Roy S (eds) Anthropogeomorphology of bhagirathi-hooghly river system in India. Routledge, pp 331–356

Patel PP, Dasgupta R, Chanda S, Mondal S (2021) An investigation into longitudinal forms of gullies within the "Grand Canyon" of Bengal Eastern India. Transactions in GIS. https://doi.org/10.1111/tgis.12828

Pike RJ (2001) Topographic fragments of geomorphometry, GIS, and DEMs. In DEMS and Geomorphology, Geographic Information Systems Association (Japan) Special Publication. 5th International Conference on Geomorphology, Chuo University: Tokyo, Japan (Vol. 1, pp. 34–35)

Pike RJ, Wilson SE (1971) Elevation-relief ratio, hypsometric integral, and geomorphic area-altitude analysis. Geol Soc Am Bull 82(4):1079–1084

Qin CZ, Zhu AX, Pei T, Li BL, Scholten T, Behrens T, Zhou CH (2011) An approach to computing topographic wetness index based on maximum downslope gradient. Precision Agric 12(1):32–43. https://doi.org/10.1007/s11119-009-9152-y

Riebsame WE, Meyer WB, Turner BL (1994) Modeling land use and cover as part of global environmental change. Clim Change 28(1–2):45–64. https://doi.org/10.1007/BF01094100

Rodriguez-Iturbe I, Escobar LA (1982) The dependence of drainage density on climate and geomorphology. Hydrol Sci J 27(2):129–137

Saha D, Das D, Dasgupta R, Patel PP (2020) Application of ecological and aesthetic parameters for riparian quality assessment of a small tropical river in eastern India. Ecol Ind 117:106627. https://doi.org/10.1016/j.ecolind.2020.106627

Sarkar A, Patel PP (2011) Topographic analysis of the Dulung R. Basin. Indian J Spatial Sci **II**(1, Article 2)

Sarkar A, Patel PP (2012) Terrain classification of the Dulung drainage basin. Indian J Spatial Sci III(1, Article 6)

Sarkar A, Patel PP (2016) Land use—terrain correlations in the piedmont tract of eastern India: a case study of the Dulung river basin. In: Santra A, Mitra S (eds) Handbook of research on remote sensing applications in earth and environmental studies, IGI Global, USA, pp 147–193. DOI: https://doi.org/10.4018/978-1-5225-1814-3.ch008

Schumm SA (1956) Evolution of drainage systems and slopes in badlands at Perth Amboy, New Jersey. Geol Soc Am Bull 67(5):597–646

Shreve RW (1969) Stream lengths and basin areas in topologically random channel networks. J Geol 77:397–414

Singh RL (1975) Regional geography of India. National Geographical Society of India (Banaras Hindu University. Dept. of Geography. Varanasi. India), 654–655

Singh P, Gupta A, Singh M (2014) Hydrological inferences from watershed analysis for water resource management using remote sensing and GIS techniques. Egypt J Remote Sens Space Sci 17:111–121

Smith KG (1958) Erosional processes and landforms in Badlands national monument South Dakota. Bull Geol Soc 69:975–1008

Smith GH (1935) The relative relief of Ohio. Geogr Rev 25(2):272–284

Smith KG (1950) Standards for grading texture of erosional topography. Am J Sci 248(9):655–668

Soni S (2017) Assessment of morphometric characteristics of Chakrar watershed in Madhya Pradesh India using geospatial technique. Appl Water Sci 7:2089–2102. https://doi.org/10.1007/s13201-016-0395-2

Strahler AN (1952) Hypsometric (area-altitude) analysis of erosional topography. Geol Soc Am Bull 63(11):1117–1142

Strahler AN (1954) Statistical analysis in geomorphic research. J Geol 62(1):1–25

Strahler AN (1957) Quantitative analysis of watershed geomorphology. EOS Trans Am Geophys Union 38(6):913–920

Strahler AN (1964) Part II. Quantitative geomorphology of drainage basins and channel networks. Handbook of Applied Hydrology: McGraw-Hill, New York, 4–39

Subramanyan V (1981) Geomorphology of the Deccan volcanic province. Memoir-Geol Soc India 3:101–116

Sutradhar H (2020) Assessment of drainage morphometry and watersheds prioritization of Siddheswari River Basin, eastern India. J Indian Soc Remote Sens 1–18. https://doi.org/10.1007/s12524-020-01108-5

Szabo J (2006) Anthropogenic geomorphology: subject and system. In: Szabo J, David L, Loczy D (eds) Anthropogenic geomorphology: a guide to man-made landforms. Springer, Dordrecht, pp 3–12

Tagil S, Jenness J (2008) GIS-based automated landform classification and topographic, landcover and geologic attributes of landforms around the Yazoren Polje, Turkey. J Appl Sci 8:910–921

Tobler W (2000) The development of analytical cartography: a personal note. Cartogr Geogr Inf Sci 27(3):189–194

Tucker GE, Bras RL (1998) Hillslope processes, drainage density, and landscape morphology. Water Resour Res 34(10):2751–2764

Turner B, Moss RH, Skole DL (1993) Relating land use and global land-cover change. IGBP Report # 24/HDP Report #5. Stockholm

Vaidya N, Kuniyal JC, Chauhan R (2013) Morphometric analysis using Geographic Information System (GIS) for sustainable development of hydropower projects in the lower Satluj river catchment in Himachal Pradesh, India. Int J Geomat Geosci 3(3):464–473

Vijith H, Satheesh R (2006) GIS based morphometric analysis of two major upland sub-watersheds of Meenachil river in Kerala. J Indian Soc. Remote Sens 34(2):181

Wasson RJ (1994) Annual and decadal variation of sediment yield in Australia, and some global comparisons. IAHS Publications-Series of Proceedings and Reports-Intern Assoc Hydrological Sciences 224:269–280

Weiss AD (2000) Topographic position and landforms analysis. Poster http://www.jennessent.com/downloads/tpi-poster-tnc_18x22.pdf

Weiss AD (2001) Topographic position and landforms analysis. Poster Presentation, ESRI Users Conference, San Diego, CA

Wentworth CK (1930) A simplified method of determining the average slope of land surfaces. Am J Sci 117:184–194

Wilson JP, Gallant JC (2000) Primary topographic attributes. In: Wilson JP, Gallant JC (eds) Terrain analysis: principles and applications. John Wiley and Sons, pp 51–85

Wise S (2000) Assessing the quality for hydrological applications of digital elevation models derived from contours. Hydrol Process 14(11–12):1909–1929

Yokoyama H, Watanabe Y, Shimizu Y, Bousmar D, Zech Y (2002, September) Numerical simulation of sandbars using 2-D shallow water equation under unsteady flow. In River flow 2002. Proceedings of the international conference on fluvial hydraulics. Louvain-La-Neuve, Belgium (pp. 4–6)

Zhang Y (2005) Global tectonics and climatic control of mean elevation of continents and Phanerozoic sea level change. Earth Planet Sci Lett 237:524–531. https://doi.org/10.1016/j.epsl.2005.07.015